Am J Cancer Res 2023;13(12):5868-5886
www.ajcr.us /ISSN:2156-6976/ajcr0152070

Original Article

EIF4A3 induced circGRIK2 promotes the malignancy of glioma by regulating the miR-1303/HOXA10 axis

Fubin Li[1], Wei Song[2], Lin Wu[3], Bin Liu[4], Xinrui Du[1]

[1]Department of Neurosurgery, Zibo Central Hospital, Zibo 255036, Shandong, China; [2]Department of Breast and Thyroid Surgery, Zibo Central Hospital, Zibo 255036, Shandong, China; [3]Department of Pediatrics, Zhangdian Maternal and Child Health Care Hospital, Zibo 255036, Shandong, China; [4]Department of Critical Care Medicine, Shandong Provincial Hospital Affiliated to Shandong First Medical University, Jinan 250021, Shandong, China

Received July 6, 2023; Accepted November 13, 2023; Epub December 15, 2023; Published December 30, 2023

Abstract: In recent years, the role of circular RNAs (circRNAs) in glioma has become increasingly important. However, there are still many newly discovered circRNAs with unknown functions that require further study. In this study, circRNA sequencing, qPCR, MTS, EdU, Transwell, and other assays were conducted to detect the expression and malignant effects of a novel circRNA molecule, circGRIK2, in glioma. qPCR, western blotting, RIP, and luciferase reporter gene experiments were used to investigate the downstream molecular mechanisms of circGRIK2. Our study found that circGRIK2 was highly expressed in glioma and promoted glioma cell viability, proliferation, invasion, and migration. Mechanistically, circGRIK2 acted as a competitive sponge for miR-1303, upregulating the expression of HOXA10 to exert its oncogenic effects. Additionally, the RNA-binding protein EIF4A3 could bind to and stabilize circGRIK2, leading to its high expression in glioblastoma. The discovery of circGRIK2 in this study not only contributes to a better understanding of the biological mechanisms of circGRIK2 in glioma but also provides a new target for molecular targeted therapy.

Keywords: Glioma, circGRIK2, miR-1303, HOXA10, EIF4A3

Introduction

Glioma is a malignant tumor that originates from glial cells in the brain. It includes various types, such as astrocytoma, oligodendroglioma, ependymoma, and glioblastoma [1]. The treatment methods for glioma include surgical resection, radiation therapy, and chemotherapy. Individualized treatment plans are usually developed based on the tumor type, location, and overall condition of the patient [2]. Surgical resection aims to remove as much tumor tissue as possible, while radiation therapy and chemotherapy are used to reduce or control the growth and spread of remaining tumor cells [3]. However, the overall effectiveness of these combined treatments is not ideal, and glioblastoma, the most malignant form of glioma, is particularly prone to recurrence. Even with aggressive surgery and chemoradiotherapy, the median survival time for patients with glioblastoma is less than 15 months, posing a significant threat to patient's life expectancy and quality of life [4]. In recent years, with advances in the understanding of the mechanisms underlying tumor development, numerous genetic molecules have been identified to be involved in the occurrence and progression of malignant tumors, leading to the concept of targeted molecular therapy for cancer [5]. Therefore, exploring genes associated with tumor development has become a new direction in basic and clinical research on treatment.

Circular RNAs (circRNAs) are a type of noncoding RNA molecules that form a closed-loop structure. Unlike linear RNAs, circRNAs are formed by the covalent linkage of the 3' and 5' ends, creating a circular structure that exhibits relative stability [6]. Initially, circRNAs were considered byproducts of RNA processing and splicing and were thought to be nonfunctional [7]. However, as research progresses, it has been discovered that circRNAs play important

functional roles in various biological processes and are involved in the development of several diseases. In recent years, circRNAs have also garnered significant attention in the context of cancer. Some circRNAs are overexpressed in tumors and are associated with processes such as proliferation, invasion, and metastasis [8]. For example, circKPNB1 is highly expressed in glioma and promotes the proliferation and self-renewal of glioma stem cells by activating the TNF-α/NF-κB signaling pathway [9]. CircLRFN5 is downregulated in glioblastoma and induces ferroptosis through the PRRX2/GCH1 pathway, inhibiting the malignant progression of the tumor. Therefore, circRNAs are considered potential tumor markers and therapeutic targets [10]. Although some studies have reported the biological roles of circRNAs in glioma, there is still a vast number of functionally unknown circRNAs that require further in-depth research.

Circular RNAs exert their functions through various mechanisms, with one of the most common mechanisms being their ability to act as "sponges" for microRNAs (miRNAs), thereby regulating the expression of downstream genes [11]. CircRNAs can contain multiple binding sites for miRNAs and interact with them, inhibiting miRNA binding to other target genes and thereby regulating gene expression [12]. This regulatory mechanism is known as competitive endogenous RNA (ceRNA) action. For example, circPTPRF promotes the progression of glioblastoma by sponging miR-1208 to upregulate YY1 [13]. CircRNA-104718 promotes glioma malignancy by regulating the miR-218-5p/HMGB1 signaling pathway [14].

In this study, we discovered a novel circular RNA molecule, circGRIK2 (hsa_circ_0077500), which exhibits abnormal overexpression in glioma. Through cellular and nude mouse experiments, we confirmed its role in promoting glioma cell proliferation, invasion, and tumorigenesis. Mechanistically, circGRIK2 acted as a sponge for miR-1303, thereby inhibiting its function and reducing the suppression of HOXA10. HOXA10, as a transcription factor and oncogene, plays a role in promoting malignant progression of glioma cells. Therefore, circGRIK2 was identified as a newly discovered oncogene in glioma, and it holds promise as an important target for molecular targeted therapy of glioma.

Materials and methods

Clinical specimens

This study was approved by the Ethics Committee of the Zibo Central Hospital, and all subjects provided informed consent before surgery. A total of 35 glioma samples were collected from January 2019 to November 2022. Among them, ten cases were WHO grade II, ten cases were WHO grade III, and 15 cases were WHO grade IV. Another ten glioma samples with adjacent normal brain tissues were collected for comparison between glioma and normal brain tissue.

Cell treatment

The U87, U251, and T98G glioma cell lines were acquired from the Cell Center of the Chinese Academy of Sciences in Shanghai, China. The U118 glioma cell line and normal human astrocytes were purchased from iCell Bioscience in Shanghai, PR China. The LN229 glioma cell line was acquired from American Type Culture Collection (ATCC) in Manassas, VA, USA. All glioma cell lines were cultured in Dulbecco's modified Eagle's medium (DMEM) from HyClone in Logan, UT, USA, supplemented with 10% fetal bovine serum (FBS) from Gibco in Carlsbad, CA, USA, and 1% penicillin/streptomycin from Gibco at 37°C with 5% CO_2.

Transfection

The pLVX vector (obtained from GenePharma Co., Ltd., Shanghai, China) was used to construct the circGRIK2 and GRIK2 overexpression plasmids. To silence circGRIK2 expression, two small interfering RNAs (siRNAs; obtained from GenePharma) targeting circGRIK2 were employed. The sequence for circGRIK2-KD1 was 5'-GGCACTCCCATGGAAAGCTGA-3', and that for circGRIK2-KD2 was 5'-CTCCCATGGAAAGCTGACCTT-3'. Additionally, circGRIK2-NC had the sequence 5'-AACAGUCGCGUUUGCGACUGG-3'. Thermo Fisher Scientific (Waltham, MA, USA) provided the mimic, inhibitor, and negative control of miR-1303 (Assay IDs: MC17558 and MH17558). To select transfected glioma cells, puromycin (Sigma, Santa Clara, CA, USA) was applied at a concentration of 10 μg/ml for 15 days. The transfection efficiency was verified using qPCR or western blotting.

Quantitative real-time polymerase chain reaction (qPCR)

Total RNA was extracted from glioma cells using the TRIzol reagent (Invitrogen, Carlsbad, CA, USA). A TaqMan reverse transcription kit (Thermo Fisher Scientific) was utilized to perform reverse transcription and generate complementary DNA (cDNA). For qPCR assays, cDNAs were treated with the Power SYBR Green master mix (Applied Biosystems, Foster City, CA, USA) or TaqMan microRNA assays (Thermo Fisher Scientific, Inc.). The relative expression of RNAs was determined using the 2-ΔΔCt method, with the β-actin gene serving as the internal reference. The sequences of the primers used were as follows: circGRIK2: forward 5'-ACACAGATTGGCGGCCTTAT-3' and reverse 5'-AGGGCTTGGAAAAGTCGATGA-3'; GRIK2: forward 5'-TTCAGGCGCACCGTTAAACT-3' and reverse 5'-GCTCCCATTGGGCCAGATT-3'; β-actin: forward 5'-TGGGACAGCCTCTACCCTTAG-3' and reverse 5'-GTCAAGGTCCCTGAGCTGAA-3'; HOXA10: forward 5'-CTCGCCCATAGACCTGTGG-3' and reverse 5'-GTTCTGCGCGAAAGAGCAC-3'.

RNase R assay

After extracting total RNA from glioma cells, it was treated with the RNase R enzyme (Geneseed, Guangzhou, China) at a concentration of 20 U/μL, followed by incubation at 37°C for 30 minutes. Subsequently, the total RNA was evaluated by qPCR.

Western blotting

Total protein was extracted from glioma cells using protein lysis buffer (Beyotime Biotechnology, Beijing, China). Equal amounts of protein samples were then loaded onto a 10% sodium dodecyl sulfate-polyacrylamide gel for electrophoresis. The proteins from the gels were subsequently transferred onto nitrocellulose membranes, which were blocked with 2% bovine serum albumin (Beyotime Biotechnology). Next, the membranes were incubated overnight at 4°C with either an anti-HOXA10 or anti-β-actin antibody (Abcam, Shanghai, China), followed by incubation on the next day with a secondary antibody (Abcam). Finally, the protein bands were visualized using an enhanced chemiluminescence (ECL) detection kit (Beyotime Biotechnology), and the ImageJ software (National Institutes of Health, Bethesda, MD, USA) was used to quantify the band densities.

Cell counting kit-8 (CCK-8) assay

Glioma cells in the exponential growth phase were seeded into 96-well plates at a density of 1×10^3 cells/100 μL/well, with four replicate wells per group. Subsequently, the cells were treated with 10 μL of the CCK-8 solution (Beyotime Biotechnology) for 2 hours on Days 1, 2, 3, 4, and 5. The absorbance (A) value of each well was measured at 450 nm using a microplate reader.

5-Ethynyl-2'-deoxyuridine (EdU) proliferation assay

Glioma cells in the exponential growth phase were seeded into 24-well plates at a density of 1×10^5 cells per well and incubated for 24 hours. Afterward, the cells were treated with the EdU reagent (Beyotime Biotechnology) at 37°C for 2 hours. Next, the cells were fixed using paraformaldehyde, and the nuclei were stained with DAPI (Sigma). The EdU-positive cells were then observed, and images were captured using a laser scanning confocal microscope (Olympus, Tokyo, Japan).

Transwell and migration assays

For the Transwell assay, the upper chamber (pore size: 8 μm) of the Transwell system was coated with 100 μl of Matrigel (BD Biosciences, CA, USA), followed by incubation at 37°C for 30 minutes. Subsequently, glioma cells in the exponential growth phase were seeded into the upper chamber in DMEM supplemented with 0.2% FBS, while the lower chamber contained DMEM supplemented with 20% FBS. After 20 hours of incubation, cells in the lower chamber were fixed using 4% paraformaldehyde and stained with hematoxylin and eosin (H&E). The number of invasive glioma cells was then counted under an inverted microscope (Olympus). For the migration assay, glioma cells were directly seeded into the upper chamber, without Matrigel coating. The subsequent steps were similar to those of the Transwell assay.

Luciferase activity analysis

The binding sites between miR-1303 and circGRIK2 were predicted using the circInterac-

tome database (https://circinteractome.nia.nih.gov). Similarly, the binding sites between miR-1303 and HOXA10 were predicted using the starBase database (https://starbase.sysu.edu.cn). Subsequently, wild-type circGRIK2, mutant circGRIK2, wild-type HOXA10, and mutant HOXA10 sequences were designed, cloned and inserted into the empty pmirGLO luciferase reporter vector from Promega. These constructs were then transfected into glioma cells. Finally, the luciferase activity was measured using a luciferase reporter assay system from Promega.

RNA immunoprecipitation (RIP) assay

To investigate the interaction between circGRIK2 and miR-1303, we utilized the Magna RIP RNA-binding protein immunoprecipitation kit (Millipore, Darmstadt, Germany) following the manufacturer's guidelines. Glioma cells were lysed using the RIP lysis buffer, and magnetic beads were employed, along with an antibody against Ago2 or IgG (as a negative control) for immunoprecipitation. The RNA fragments bound to Ago2 were then purified and incubated with proteinase K. Finally, the enrichment of circGRIK2 and miR-1303 was detected using qPCR.

Immunohistochemistry (IHC)

Xenograft tumor specimens from mice were first embedded in paraffin and then cut into 4-μm sections. These paraffin-embedded sections were subsequently dewaxed, rehydrated, and subjected to antigen retrieval. To block endogenous peroxidases, an immunohistochemistry kit from Beyotime Biotechnology was used. The sections were then incubated with a primary antibody against Ki-67 or HOXA10 (dilution 1:100; Abcam). Staining was performed using the DAB substrate kit from Abcam. The stained sections were observed under a light microscope (Olympus), and the immunohistochemical results were evaluated using the German immunohistochemical score [15].

Xenograft experiments

Female BALB/c nude mice (Shanghai SLAC Laboratory Animal Co., Ltd., Shanghai, China) aged 6 weeks were used for orthotopic injection of glioma cells in the exponential growth phase. Each mouse received an injection of 1×10^4 glioma cells. The mice were then monitored daily for signs of neurological symptoms or death. The tumor volume was calculated using the following formula: $V = (D \times d^2)/2$, where D represents the longest tumor diameter and d represents the shortest tumor diameter. Survival rates were analyzed using the log-rank test and Kaplan-Meier analysis. All animal experiments were conducted in accordance with the guidelines of the Animal Care Committee of the Zibo Central Hospital.

Bioinformatic analyses

Candidate miRNAs for circGRIK2 were predicted using the circInteractome database (https://circinteractome.nia.nih.gov) and the Cancer-Specific CircRNA Database 2.0 (CSCD, http://geneyun.net/CSCD2/#). Candidate mRNAs for miR-1303 were predicted using miRPathDb 2.0 (https://mpd.bioinf.uni-sb.de/overview.html), miRWalk (http://mirwalk.umm.uni-heidelberg.de), TargetScan (http://www.targetscan.org/vert_71/), MiRDB (http://mirdb.org), and starBase (starbase.sysu.edu.cn).

Statistical analysis

Statistical analysis and visualization were conducted using GraphPad Prism 8.0 (GraphPad Software, Inc., San Diego, CA, USA). Each experiment was repeated at least three times, and the results are presented as the mean ± standard error. The chi-square test, F test, or t test was applied for group comparisons as appropriate. Statistical significance was defined as a P value < 0.05.

Results

CircGRIK2 expression is highly enriched in glioma tissues and cells

To analyze differences in the expression of circRNAs in glioma, we performed circRNA sequencing on 3 glioma tissues and 3 adjacent normal brain tissues (NBTs). The results were analyzed using the limma differential gene analysis, with screening criteria of $\log2|FC| > 1$ and a p value < 0.05. A total of 1626 circRNAs showed differential expression. As shown in the volcano and differential expression ranking plots, 929 circRNAs were upregulated and 697 circRNAs were downregulated in glioma tissues

compared with the adjacent NBTs (**Figure 1B**, **1C**). The heatmap displays the top 30 significantly dysregulated circRNAs, among which circGRIK2 (hsa_circ_0077500) was identified as one of the most significantly expressed circRNAs in glioma (**Figure 1A**). **Figure 1D** and **1E** reveal the basic information on circGRIK2. It is derived from the 6th chromosome, with a genomic location of chr6:102337514-102483441, and is formed by back-splicing of four exons (exons 14-17) of the GRIK2 gene. Sanger sequencing demonstrated that circGRIK2 could form a closed loop, with the junction site being G-A (**Figure 1F**). Fluorescence in situ hybridization (FISH) experiments indicated its localization in the cytoplasm of glioma cells (**Figure 1G**). Considering the stability of its circular structure and resistance to RNase degradation, we found that the expression levels of circGRIK2 in U118 and A172 glioma cells remained unchanged after RNase treatment, while the expression of the linear RNA GRIK2 was significantly downregulated (**Figure 1H**, **1I**). We further examined the expression of circGRIK2 in glioma tissues and found that it was significantly upregulated compared to adjacent NBTs. Moreover, its expression further increased with higher WHO grades, with the highest expression observed in grade IV glioma (**Figure 1J**, **1K**). Additionally, we detected circGRIK2 expression in various glioma cell lines and normal human astrocytes (NHAs) and found that the expression of circGRIK2 was significantly higher in glioma cell lines than in NHAs (**Figure 1L**). These findings indicate that circGRIK2 exhibits significantly elevated expression in both glioma tissues and glioma cell lines, suggesting its potential involvement in the development of glioma.

CircGRIK2 overexpression promoted proliferation and invasion of glioma cells

To further explore the biological role of circGRIK2 in glioma, we overexpressed circGRIK2 in glioma cell lines and observed its effects on cell proliferation, invasion, and other biological functions. Based on the results shown in **Figure 1L**, we found that circGRIK2 expression was the lowest in the U87 and T98G cell lines; therefore, these two cell lines were used for overexpression. qPCR confirmed the efficient and reliable overexpression of circGRIK2 in U87 and T98G cells (**Figure 2A**). The MTS assay revealed that U87 and T98G cells had higher absorbance values after circGRIK2 overexpression, indicating increased cell viability (**Figure 2B**, **2C**). The EdU experiments showed a higher percentage of EdU-positive cells in U87 and T98G cells after circGRIK2 overexpression, confirming their enhanced cell proliferation capabilities (**Figure 2D**). The Transwell and migration assays demonstrated significant increases in the numbers of invaded and migrated U87 and T98G cells after circGRIK2 overexpression, supporting the notion that circGRIK2 overexpression significantly promotes glioma cell invasion and migration (**Figure 2E**, **2F**). Therefore, the above results indicate that circGRIK2 overexpression promotes glioma cell viability and proliferation, enhances invasion and migration capabilities, and contributes to the biological effects associated with malignant progression.

CircGRIK2 knockdown promoted the proliferation and invasion of glioma cells

Given the aforementioned findings regarding the proproliferative and invasive effects of circGRIK2 overexpression in glioma cells, we next silenced circGRIK2 expression in the U118 and A172 glioma cell lines. qPCR confirmed the reliable and significant silencing efficiency of circGRIK2 posttransfection (Supplementary Figure 1A). Using the MTS (Supplementary Figure 2A, 2B), EdU (Supplementary Figure 2C), Transwell (Supplementary Figure 2D), and migration (Supplementary Figure 2E) assays, we observed that circGRIK2 silencing effectively inhibited glioma cell viability and proliferation and decreased invasion and migration capabilities. These results again confirm that circGRIK2 contributes to the biological effects associated with malignant progression.

CircGRIK2 directly targets miR-1303 in glioma cells

In view of the biological role of circGRIK2 overexpression in promoting the malignant progression of glioma cells, as revealed by the aforementioned studies, we further analyzed its possible molecular mechanisms. Since circular RNAs contain a large number of miRNA response elements (MREs) and can act as sponges to adsorb large amounts of miRNAs [11], thereby affecting the regulatory roles of miR-

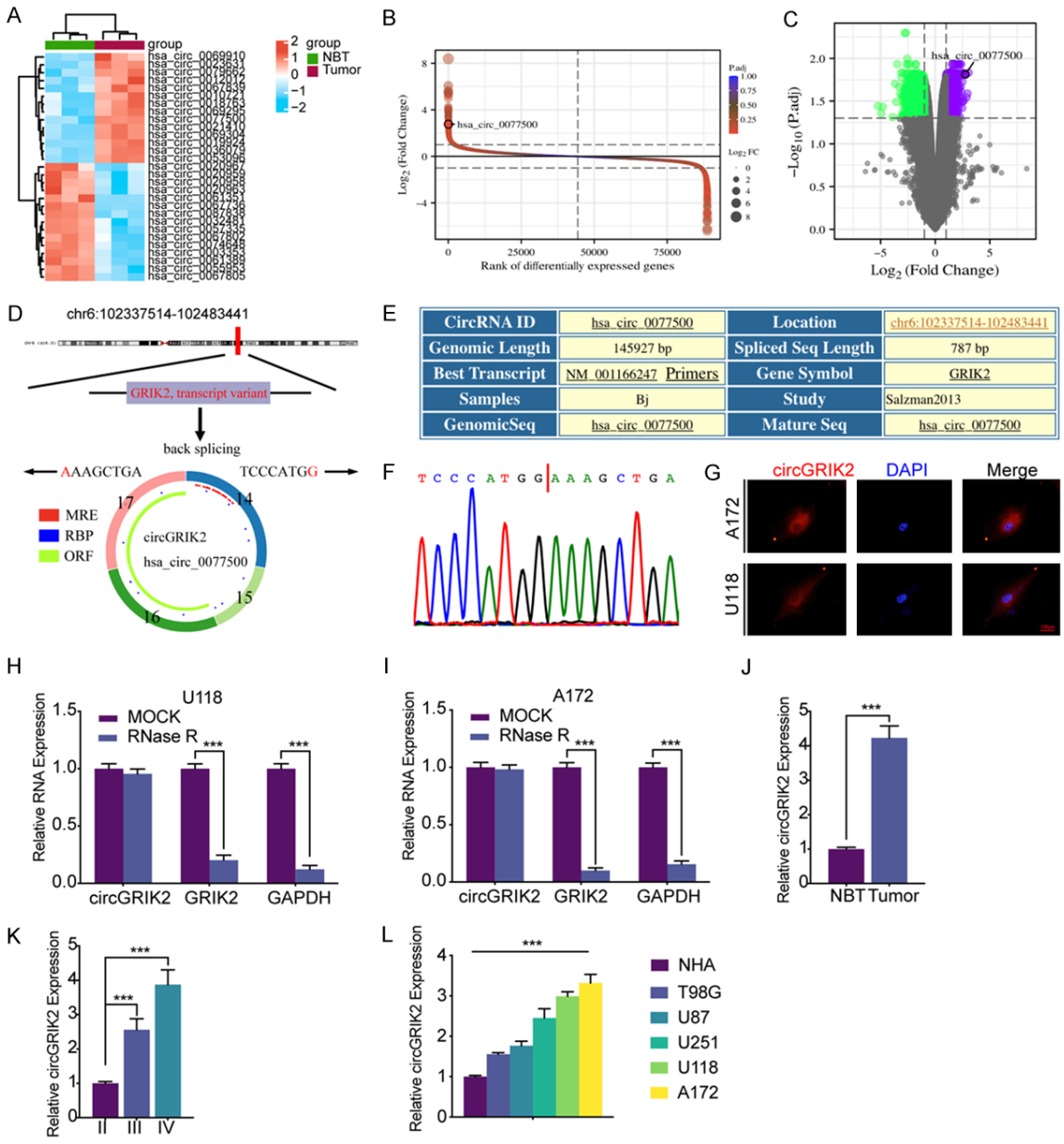

CircRNA ID	hsa_circ_0077500	Location	chr6:102337514-102483441
Genomic Length	145927 bp	Spliced Seq Length	787 bp
Best Transcript	NM_001166247 Primers	Gene Symbol	GRIK2
Samples	Bj	Study	Salzman2013
GenomicSeq	hsa_circ_0077500	Mature Seq	hsa_circ_0077500

Figure 1. CircGRIK2 expression was increased in glioma tissues and cells. (A) The heatmap displays the top 30 significantly dysregulated circRNAs, including 3 glioma tissues and 3 adjacent normal brain tissues. (B, C) The differential gene ranking plot (B) and volcano plot (C) show the expression differences of circRNAs in glioma tissues. (D) Pattern diagram of CircGRIK2. (E) The circInterome database reveals the basic information of circGRIK2. (F) Sanger sequencing reveals the reverse circularization and junction sites of circGRIK2. (G) Fluorescence in situ hybridization experiments reveal the distribution of circGRIK2 in glioma cell lines A172 and U118. (H, I) RNase experiments confirm the resistance of circGRIK2 to RNase treatment in glioma cell lines A172 and U118. Scale bar = 100 μm. (J) qPCR detects the expression differences of circGRIK2 between ten glioma tissues and their adjacent normal brain tissues. (K) qPCR detects the expression differences of circGRIK2 among ten WHO grade II, fifteen WHO grade III, and ten WHO grade IV glioma tissues. (L) qPCR detects the expression differences of circGRIK2 among various glioma cell lines (U118, A172, U251, T98G, and U87) and normal human astrocytes (NHA). All data are shown as the mean ± SD (three independent experiments). **P < 0.05; **P < 0.01; ***P < 0.001.*

NAs on downstream target genes, we explored potential miRNAs to which circGRIK2 could bind. First, we predicted potential miRNAs to which circGRIK2 could bind using the circInteractome and CSCD databases, and the intersection of the two sets of the results revealed that

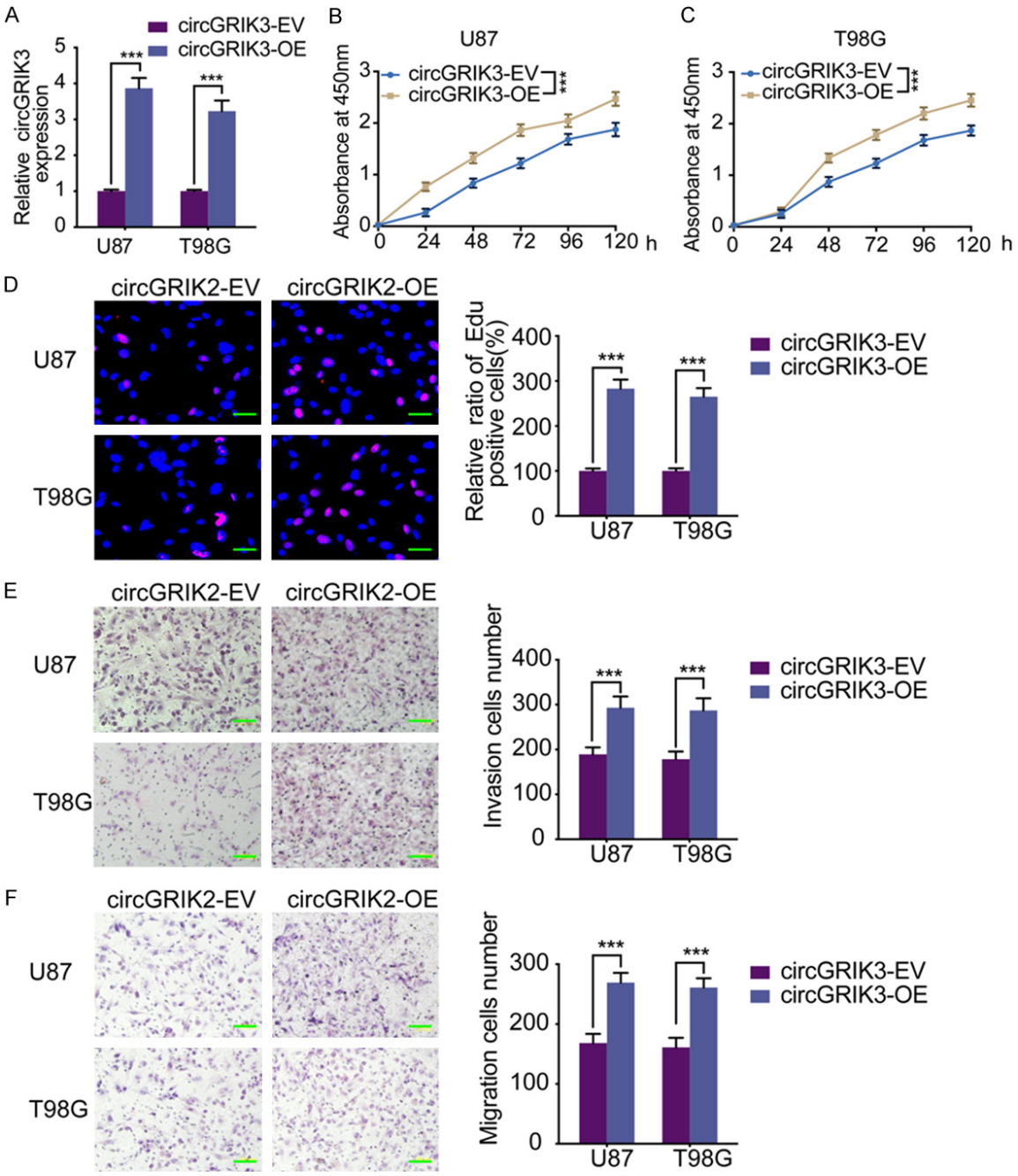

Figure 2. CircGRIK2 overexpression promoted the proliferation and invasion in glioma cells. A: qPCR assays confirmed that circGRIK2 is stably overexpressed in glioma cell lines U87 and T98G. B, C: MTS assays were performed to assess the changes in cell viability of U87 and T98G glioma cell lines after circGRIK2 overexpression. D: EdU assays were conducted to evaluate the changes in the percentage of EdU-positive cells in U87 and T98G glioma cell lines following circGRIK2 overexpression. Scale bar = 50 μm. E, F: Transwell and cell migration assays were performed to examine the alterations in the number of invaded and migrated cells in U87 and T98G glioma cell lines upon circGRIK2 overexpression. Scale bar = 50 μm. All data are shown as the mean ± SD (three independent experiments). **P < 0.05; **P < 0.01; ***P < 0.001.*

miR-1303 was the only common miRNA (**Figure 3A**). Based on the analysis of the results from the circInteractome database, we found the binding targets of circGRIK2 with miR-1303, as shown in **Figure 3B**. Initially, qPCR confirmed the transfection efficiency of the miR-1303

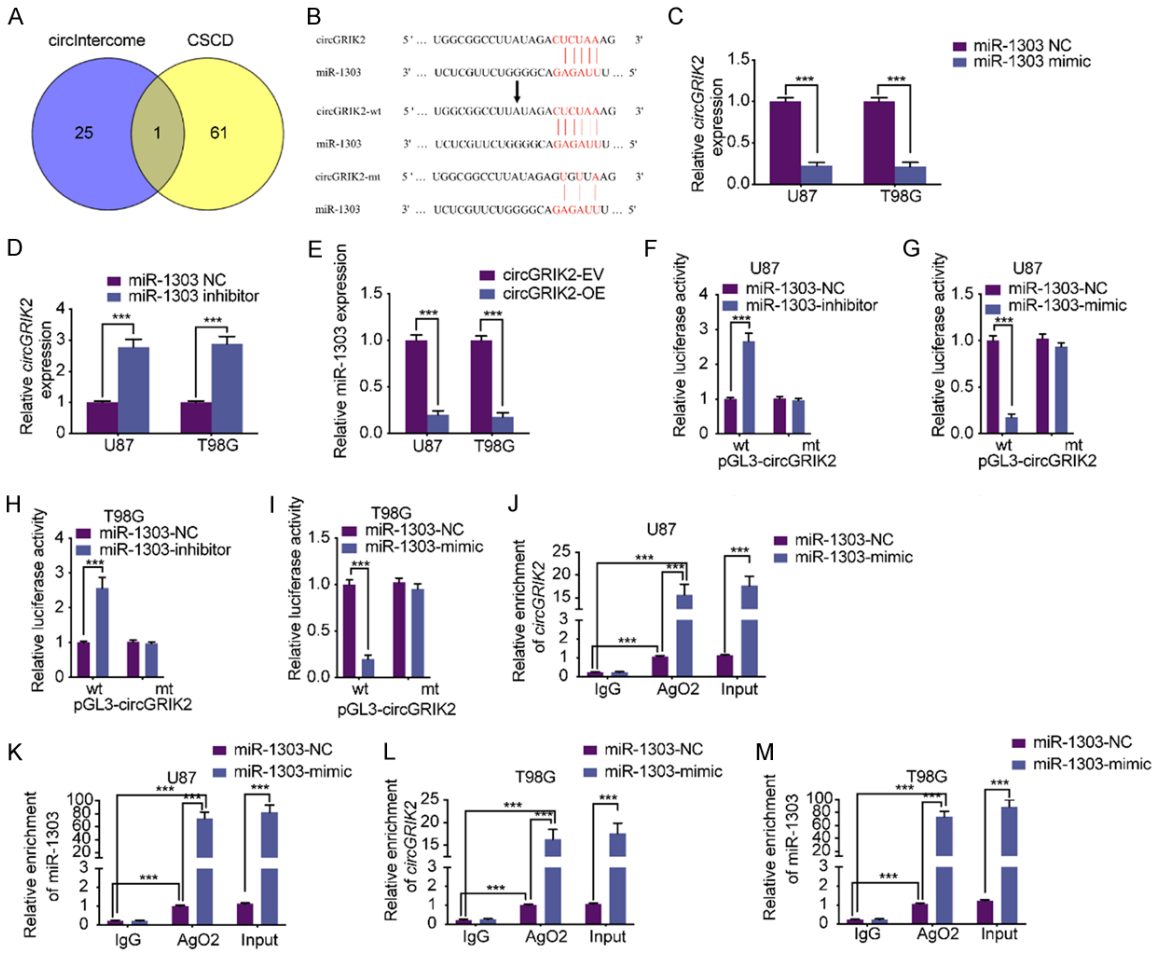

Figure 3. CircGRIK2 directly targets miR-1303 in glioma cells. A: CircIntercome database and CSCD database analysis predicted the potential miRNAs that circGRIK2 may interact with. B: CircIntercome database predicted the potential binding targets of circGRIK2 and miR-1303, along with the pattern of mutation sites. C, D: qPCR analysis was conducted to determine the expression level changes of circGRIK2 after treatment with miR-1303 mimic or miR-1303 inhibitor. E: qPCR assays revealed the expression level changes of miR-1303 in U87 and T98G cells overexpressing circGRIK2. F-I: Luciferase reporter assays were performed to analyze the changes in luciferase activity of circGRIK2 wild-type and mutant plasmid groups after transfection with miR-1303 mimic or miR-1303 inhibitor in U87 and T98G cells. J-M: Anti-AGO2 RIP experiments were conducted to analyze the enrichment levels of circGRIK2 and miR-1303 in U87 and T98G cells after treatment with miR-1303 mimic. All data are shown as the mean ± SD (three independent experiments). **P < 0.05; **P < 0.01; ***P < 0.001.*

mimic (Supplementary Figure 1B) and miR-1303 inhibitor (Supplementary Figure 1C) treatment in U87 and T98G glioma cells. Then, we observed significant downregulation of circGRIK2 expression after treatment of the U87 and T98G cell lines with the miR-1303 mimic, while treatment with the miR-1303 inhibitor resulted in significant upregulation of circGRIK2 expression (**Figure 3C**, **3D**). Furthermore, we overexpressed circGRIK2 in the U87 and T98G cell lines and detected significant decreases in the expression levels of miR-1303 (**Figure 3E**). Based on the predicted binding sites shown in **Figure 3B**, we designed mutation sites for binding and conducted luciferase reporter assays, which revealed that after treatment of U87 and T98G cells with the miR-1303 inhibitor, the wild-type group exhibited significantly higher luciferase activity of circGRIK2 than that in the mutation group (**Figure 3F**, **3H**). Conversely, after treatment of U87 and T98G cells with the miR-1303 mimic, the wild-type group showed significantly weaker luciferase activity of circGRIK2 than that in the mutation group (**Figure 3G**, **3I**). In addition, since Argonaute 2 (Ago2) is a core component of the

RNA-induced silencing complex (RISC), which is involved in mediating the degradation of RNA bound to miRNA [16], we designed an anti-Ago2 RNA immunoprecipitation assay, which revealed that both miR-1303 and circGRIK2 showed significant enrichment in the anti-AGO2 group compared to the IgG control group, and their enrichment levels further increased in the miR-1303 mimic treatment group (**Figure 3J-M**). The above research results indicate that circGRIK2 can target and bind to miR-1303, exerting a sponge-like adsorption effect.

MiR-1303 inhibitor treatment reverses the inhibitory effects of circGRIK2 silencing in glioma cells

To further confirm the biological mechanism of circGRIK2 in promoting malignant progression of glioma cell lines through sponge-like adsorption of miR-1303, we treated the circGRIK2-silenced U118 and A172 glioma cell lines with the miR-1303 inhibitor. The MTS assay was performed and showed that the absorbance values of U118 and A172 cells significantly decreased after silencing circGRIK2. Furthermore, treatment with the miR-1303 inhibitor effectively restored the decreased absorbance values (**Figure 4A**, **4B**). The EdU assay was also conducted, and it was observed that the EdU-positive rates of U118 and A172 cells significantly decreased after silencing circGRIK2. However, treatment with the miR-1303 inhibitor effectively restored the EdU-positive rates (**Figure 4C**). The Transwell and cell migration assays were also performed, and it was found that the invasion and migration of U118 and A172 cells significantly decreased after silencing circGRIK2. Nevertheless, treatment with the miR-1303 inhibitor effectively restored the invasion and migration capabilities of the cells (**Figure 4D**, **4E**). These results indicate that the oncogenic role of circGRIK2 in promoting malignant progression of glioma cells depends on the action of miR-1303.

MiR-1303 directly targets the 3'UTR of HOXA10 in glioma cells

Given that miRNAs can cause mRNA degradation or translational inhibition by binding to the 3' untranslated region (3'UTR) of target mRNAs [17], we further explored the downstream target mRNAs that could be regulated by miR-1303. We used four databases, namely, TargetScan, miRDB, miRWalk, and miRPathDB, to predict the potential target mRNAs to which miR-1303 could bind. By taking the intersection of the predictions from these four databases, we identified three mRNA targets: MAP3K5, HOXA10, and NXPE3 (**Figure 5A**). To confirm specific regulation of mRNA by miR-1303, we treated U118 and A172 cells with the miR-1303 mimic and inhibitor separately. We found that only the expression level of HOXA10 was regulated by miR-1303. Specifically, the expression of HOXA10 was significantly downregulated after treatment with the miR-1303 mimic, while it was significantly upregulated after treatment with the miR-1303 inhibitor (**Figure 5B-E**). Furthermore, western blotting revealed that the protein expression level of HOXA10 was significantly reduced after treatment with the miR-1303 mimic, whereas the opposite result was observed after treatment with the miR-1303 inhibitor (**Figure 5F-I**). Using the miRPathDB database, binding sites between miR-1303 and the 3'UTR of HOXA10 were predicted (**Figure 5L**). Based on this, we designed mutated fragments of the binding sites in the HOXA10 3'UTR and performed the luciferase reporter assay. We found that the luciferase activities in the wild-type HOXA10 group were significantly decreased after treatment with the miR-1303 mimic, while they were significantly increased after treatment with the miR-1303 inhibitor (**Figure 5J**, **5K**, **5M**, **5N**). Finally, we analyzed whether circGRIK2, combined with miR-1303, could regulate the expression of HOXA10. We conducted qPCR and western blotting assays and found that the mRNA and protein levels of HOXA10 increased after circGRIK2 overexpression, while they were significantly suppressed after treatment with the miR-1303 mimic (**Figure 5O-T**). Based on the above information, it can be concluded that miR-1303 can directly bind to the 3'UTR of HOXA10 in glioma, leading to downregulation of its expression level.

Knockdown of circGRIK2 inhibited the proliferation and invasion of glioma cells, which was reversed by HOXA10 overexpression

To further explore whether HOXA10 is involved in mediating the biological mechanisms underlying the promoting effects of circGRIK2 on glioma cell proliferation and invasion, we overexpressed HOXA10 in the circGRIK2-silenced U118 and A172 glioma cell lines. qPCR con-

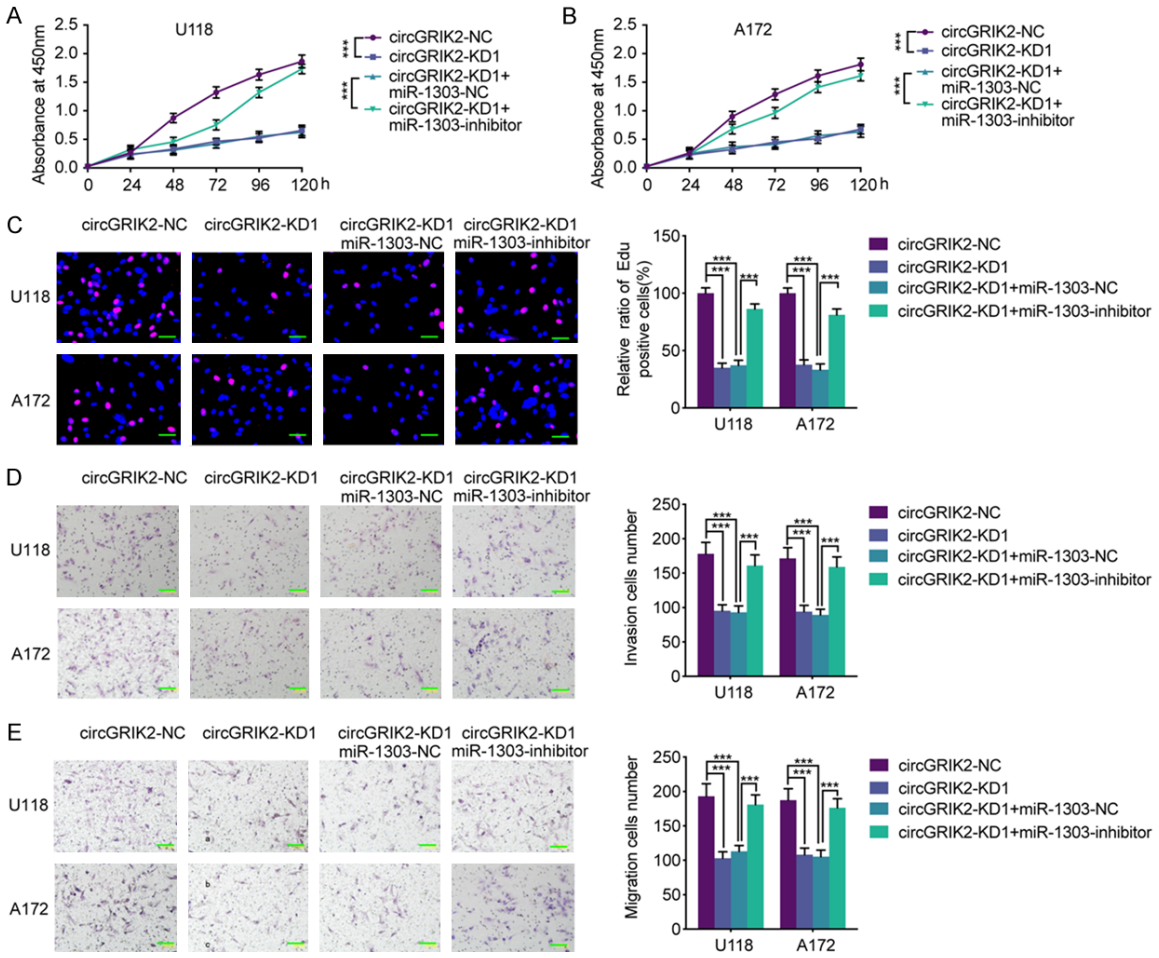

Figure 4. MiR-1303 inhibitor treatment reverses the inhibiting effects of circGRIK2 silencing in glioma cells. A, B: MTS assays were performed to observe the changes in absorbance values and cell viability in circGRIK2-silenced U118 and A172 glioma cell lines after treatment with miR-1303 inhibitor. C: EdU assays were conducted to examine the changes in the percentage of EdU-positive cells and proliferation capacity in circGRIK2-silenced U118 and A172 cells after treatment with miR-1303 inhibitor. Scale bar = 50 μm. D, E: Transwell and cell migration assays were carried out to observe the alterations in the number of invaded and migrated cells in circGRIK2-silenced U118 and A172 cells after treatment with miR-1303 inhibitor. Scale bar = 50 μm. All data are shown as the mean ± SD (three independent experiments). **P < 0.05; **P < 0.01; ***P < 0.001.*

firmed the transfection efficiency of HOXA10 and its overexpression in U118 and A172 glioma cells (Supplementary Figure 1D). The MTS assay revealed that the absorbance values of U118 and A172 cells significantly decreased after circGRIK2 silencing, while they significantly increased after HOXA10 overexpression (**Figure 6A**, **6B**). The EdU assay showed that the percentage of EdU-positive cells significantly decreased after circGRIK2 silencing in the U118 and A172 cell lines, while it significantly recovered after HOXA10 overexpression (**Figure 6C**). The Transwell and cell migration assays demonstrated that the numbers of invaded and migrated cells significantly decreased after circGRIK2 silencing in the U118 and A172 cell lines, while the numbers were effectively restored after HOXA10 overexpression (**Figure 6D**, **6E**). These results indicate that HOXA10 plays a crucial role in the promoting effects of circGRIK2 on malignant progression of glioblastoma cells.

EIF4A3 binds to and maintains the stability of circGRIK2 in glioma

In recent years, numerous studies have discovered that RNA-binding proteins (RBPs) can bind to circRNAs, thereby maintaining their stability and leading to their stably high expression in tissues [18]. To further explore the causes for the abnormally high expression of circGRIK2 in

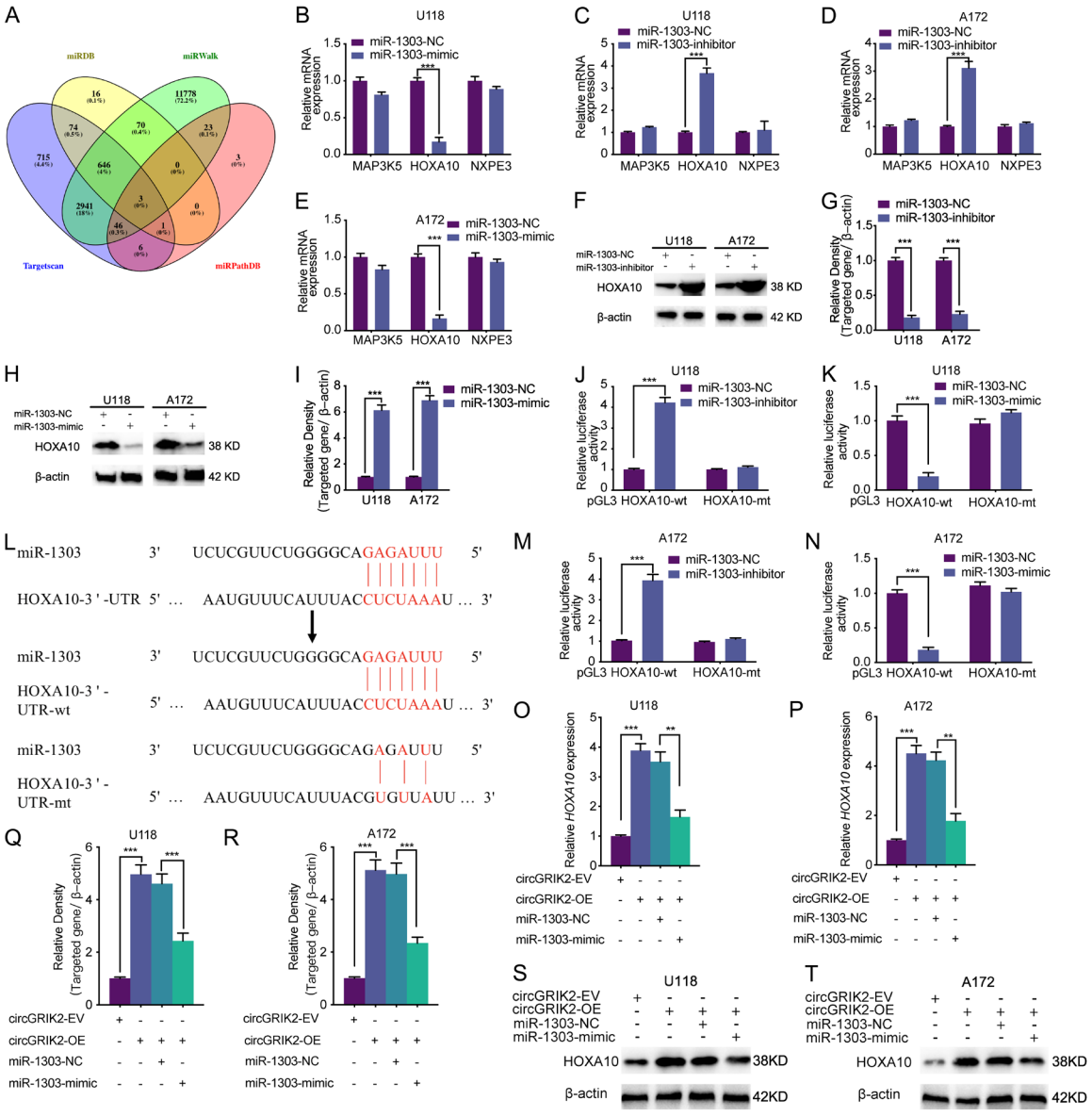

Figure 5. MiR-1303 directly targets the 3'-UTR of HOXA10 in glioma cells. (A) Targetscan, miRDB, miRWalk, and miRPathDB databases were used to predict the potential target mRNAs that miR-1303 may bind to. After taking the intersection, three mRNAs were identified: MAP3K5, HOXA10, and NXPE3. (B-E) qPCR analysis was performed to assess the mRNA level changes of MAP3K5, HOXA10, and NXPE3 in U118 and A172 cells treated with miR-1303 mimic (B, E) or inhibitor (C, D). (F-I) Western blot analysis was conducted to examine the protein level changes of HOXA10 in U118 and A172 cells treated with miR-1303 inhibitor (F, G) or mimic (H, I). (L) According to the miRPathDB database, the binding sites between miR-1303 and the 3'-UTR region of HOXA10 were predicted, and based on this, mutated fragments of the HOXA10 3'-UTR binding site were designed. (J, K, M, N) Luciferase reporter assays were performed to determine the changes in luciferase activity of HOXA10 wild-type and mutant groups after treatment with miR-1303 inhibitor or mimic. (O-T) qPCR (O, P) and western blot (Q-T) assays were conducted to assess the mRNA and protein level changes of HOXA10 in U118 and A172 cells overexpressing circGRIK2 after treatment with miR-1303 mimic. All data are shown as the mean ± SD (three independent experiments). **P < 0.05; **P < 0.01; ***P < 0.001.*

gliomas, we searched for RBPs to which circGRIK2 could bind. First, we analyzed the circInteractome and CSCD databases and identified two RBPs that intersected with circGRIK2, namely, EIF4A3 and FUS (**Figure 7A**). The numbers of binding sites of these two RBPs on circGRIK2 are shown in **Figure 7B**, indicating a higher likelihood of EIF4A3 binding to circGRIK2. The RBPsuite database showed the score of EIF4A3 binding to circGRIK2 (**Figure**

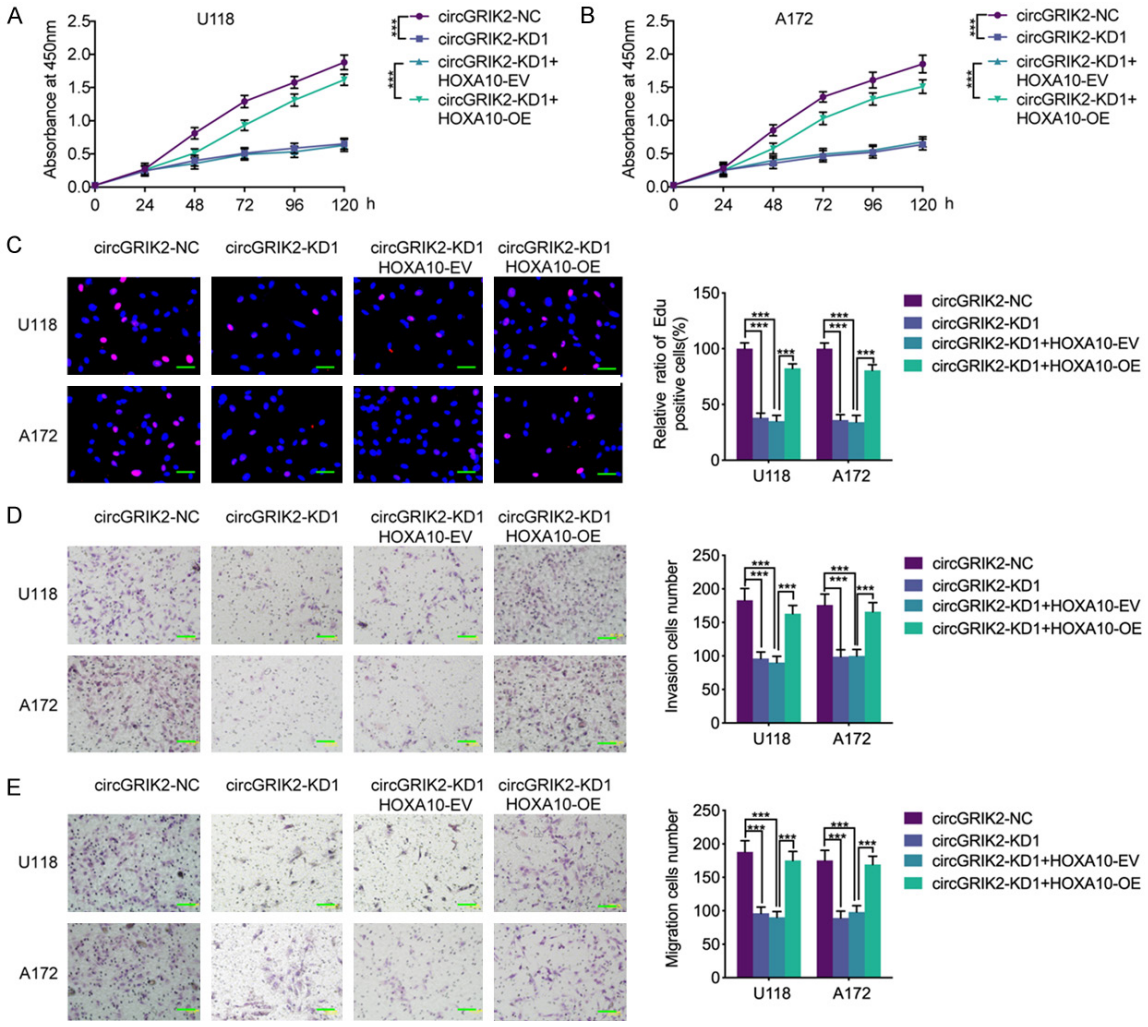

Figure 6. Knockdown of circGRIK2 inhibited proliferation and invasion in glioma cells, which was reversed by HOXA10 overexpression. A, B: MTS assays were performed to observe the changes in absorbance values and cell viability in circGRIK2-silenced U118 and A172 cells after HOXA10 overexpression. C: EdU assays were conducted to examine the changes in the percentage of EdU-positive cells and proliferation capacity in circGRIK2-silenced U118 and A172 glioma cell lines after HOXA10 overexpression. Scale bar = 50 μm. D, E: Transwell and cell migration assays were carried out to observe the alterations in the number of invaded and migrated cells in circGRIK2-silenced U118 and A172 glioma cells after HOXA10 overexpression. Scale bar = 50 μm. All data are shown as the mean ± SD (three independent experiments). **P < 0.05; **P < 0.01; ***P < 0.001.*

7C). Furthermore, we performed the RIP assay with an anti-EIF4A3 antibody and found that circGRIK2 was enriched when treated with the anti-EIF4A3 antibody. The enrichment of circGRIK2 was further increased in the circGRIK2 overexpression group, while it was significantly reduced in the circGRIK2 silencing group (**Figure 7D-G**). We overexpressed EIF4A3 in the U87 and T98G glioma cell lines and found significant increases in the expression levels of circGRIK2 (**Figure 7H**). On the other hand, the silencing of EIF4A3 in U118 and A172 cells resulted in significant decreases in the expression levels of circGRIK2 (**Figure 7I**). Finally, we conducted an actinomycin D assay and found that the half-life of circGRIK2 was significantly prolonged after EIF4A3 overexpression (**Figure 7J**, **7K**). These research findings suggest that EIF4A3 can bind to circGRIK2, maintaining its stability and resulting in significant upregulation of its expression.

CircGRIK2 promoted glioma tumorigenesis in vivo

The above experimental results confirmed at the level of glioma cell lines that circGRIK2 upregulated HOXA10 by sponge-like adsorption

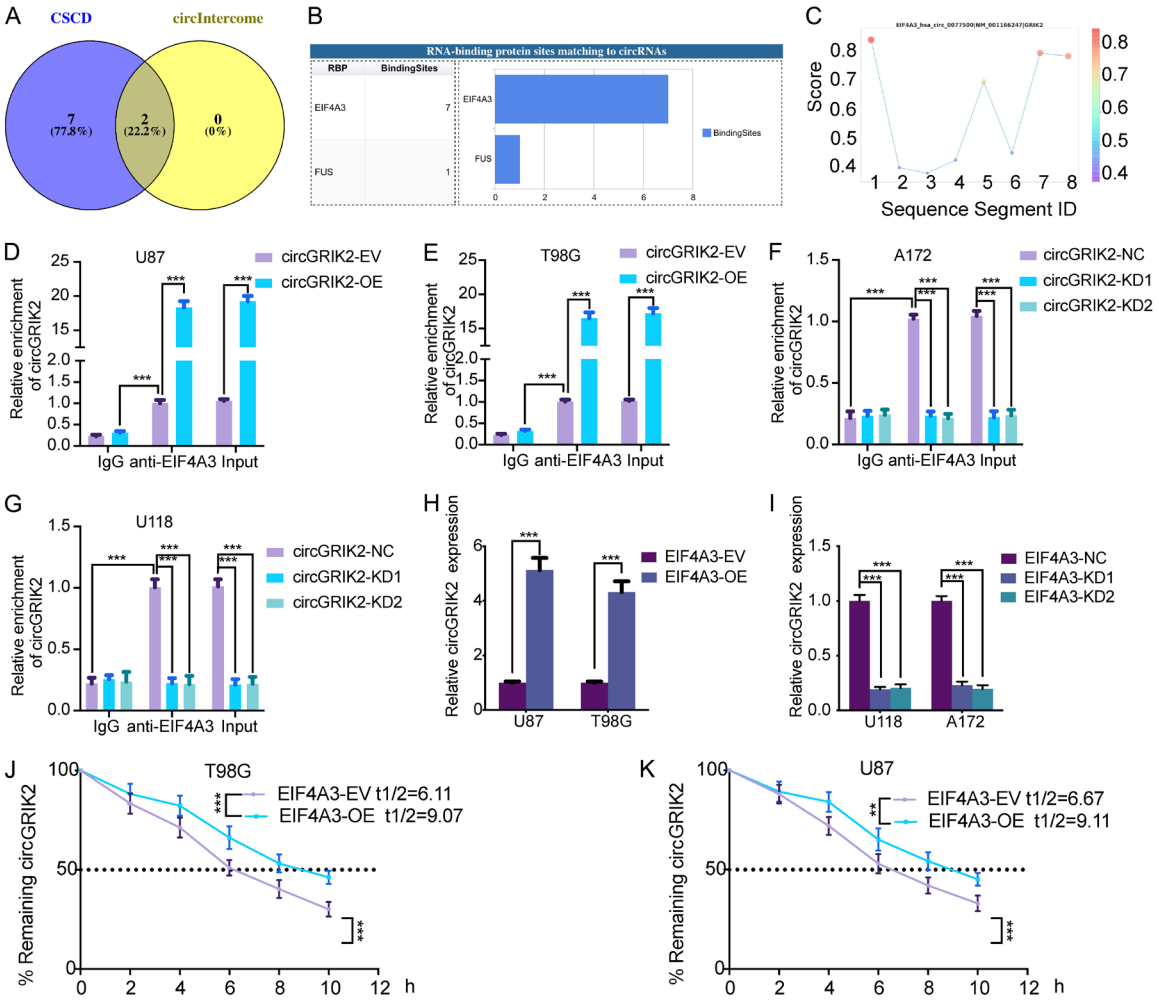

Figure 7. EIF4A3 binds to and maintains the stability of circGRIK2 in glioma. (A) CircIntercome and CSCD databases predicted the RBPs that can bind to circGRIK2, and the intersection revealed two RBPs: EIF4A3 and FUS. (B) The circIntercome database showed the number of binding targets for EIF4A3 and FUS on circGRIK2. (C) RBPsuite database displayed the binding score of EIF4A3 to circGRIK2. (D-G) RNA immunoprecipitation assays were performed to examine the enrichment levels of circGRIK2 in U118 and A172 cells overexpressing (D, E) or silencing (F, G) EIF4A3 after treatment with anti-EIF4A3 antibody and negative control (anti-IgG). (H, I) qPCR assays was conducted to determine the expression level changes of circGRIK2 after overexpression or silencing of EIF4A3. (J, K) Actinomycin D assays were performed to assess the changes in the half-life of circGRIK2 after EIF4A3 overexpression. All data are shown as the mean ± SD (three independent experiments). **P < 0.05; **P < 0.01; ***P < 0.001.*

of miR-1303, thereby promoting malignant progression, such as the proliferation, invasion, and migration, of glioma cells. We further explored whether circGRIK2 plays a role in promoting glioma tumorigenesis and development using intracranial tumor assays in nude mice. The intracranial tumor assays showed that after the implantation of the circGRIK2-overexpressing U87 glioma cell line into the brain of nude mice, the volume of the tumor formed in the brain of nude mice was significantly larger than that in the control group (**Figure 8A**, **8B**). Kaplan-Meier survival analysis revealed that the survival time of the mice in the group implanted with circGRIK2-overexpressing U87 cells was significantly shorter than that in the control group (**Figure 8C**). Immunohistochemical assays of the intracranial tumor tissue from mice showed that the staining intensity of the proliferation activity markers Ki-67 and HOXA10 was significantly higher in the circGRIK2 overexpression group than in the control

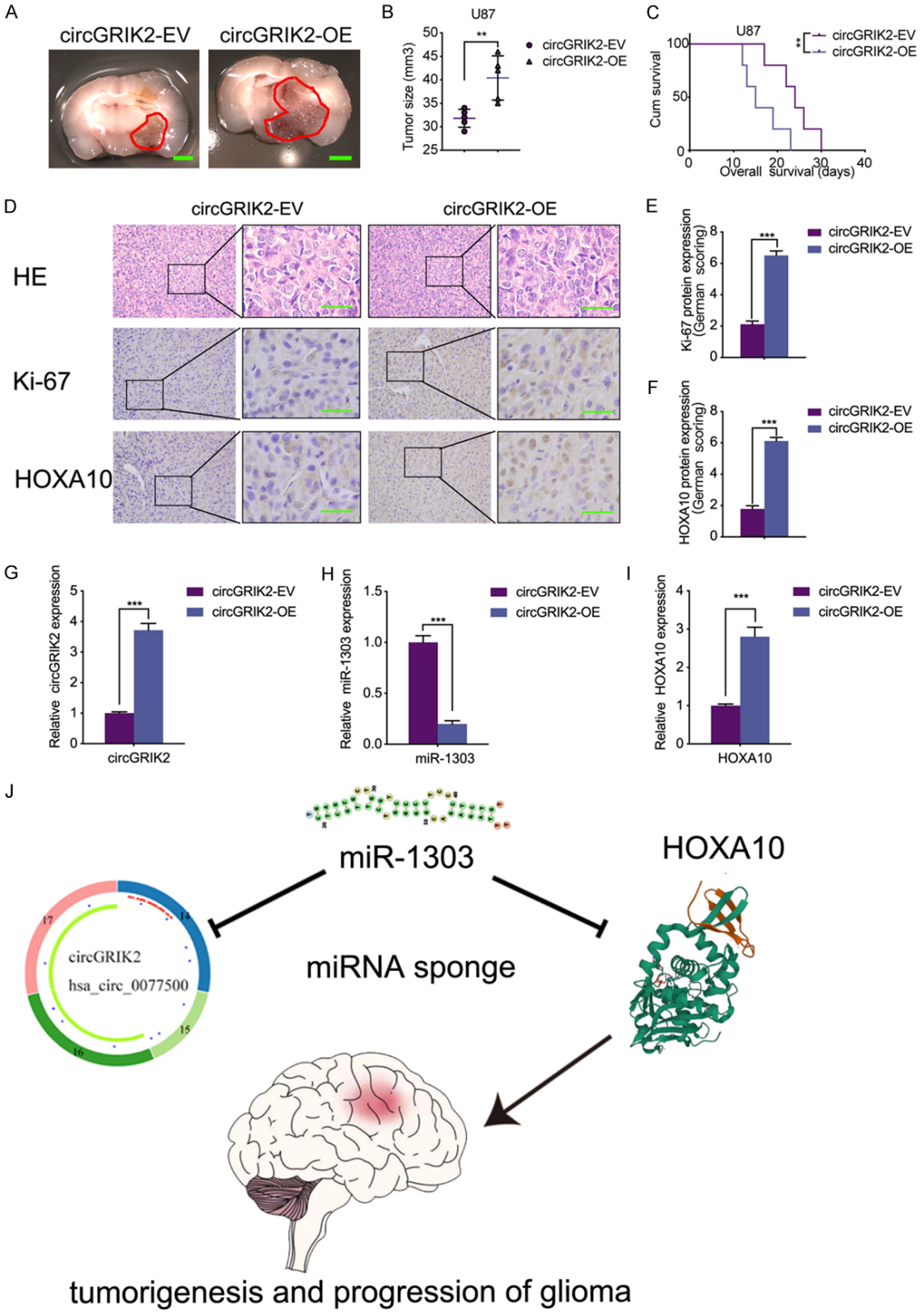

Figure 8. CircGRIK2 promoted glioma tumorigenesis in vivo. A: Representative images of tumor formation in the intracranial region of nude mice after inoculation with control or circGRIK2 overexpressed U87 cells. Scale bar = 1 mm. B: Tumor volume in the intracranial region of nude mice after inoculation with control or circGRIK2 overex-

pressed U87 cells. C: Kaplan-Meier analysis of the survival time of nude mice after inoculation with control or circGRIK2 overexpressed U87 cells. D-F: Immunohistochemical staining intensity of ki-67 and HOXA10 in tumor tissues formed in the intracranial region of nude mice. Scale bar = 50 μm. G-I: qPCR detection of the expression levels of circGRIK, miR-1303, and HOXA10 in tumor tissues. J: Schematic diagram illustrating the malignant progression effects of overexpressed circGRIK in glioma, which upregulates HOXA10 through sponge adsorption of miR-1303, thereby promoting glioma cell proliferation, invasion, and migration. All data are shown as the mean ± SD (three independent experiments). **P < 0.05; **P < 0.01; ***P < 0.001.*

group (**Figure 8D-F**). In addition, qPCR assays of the intracranial tumor tissue in nude mice revealed that the expression levels of circGRIK2 and HOXA10 were significantly increased in the circGRIK2 overexpression group, while the expression level of miR-1303 was significantly decreased (**Figure 8G-I**). The above results at the level of in vivo experiments in nude mice fully confirm the role of circGRIK2 in promoting the glioblastoma occurrence and development (**Figure 8J**).

Discussion

The treatment of gliomas typically involves a multidisciplinary approach, with an individualized treatment plan based on the location, size, and type of the tumor and the overall condition of the patient [4]. Surgery is the most common treatment for gliomas, aiming to remove as much tumor tissue as possible [2, 19]. However, complete removal of the tumor is often challenging owing to the infiltrative growth characteristics of tumor cells. Radiation therapy and chemotherapy are frequently used as adjuvant treatments following surgery to suppress tumor cell growth and recurrence and prolong patient survival [1]. Targeted therapy is a treatment method that specifically targets certain molecular targets within tumor cells [5]. Compared to traditional chemotherapy drugs, which broadly affect rapidly proliferating cells, targeted therapy drugs have greater selectivity and can interfere with specific abnormal molecules in tumor cells, thereby inhibiting tumor cell growth and metastasis [3].

Abnormal molecular signaling pathways often exist in tumor cells and are involved in important processes, such as tumor cell proliferation, survival, and angiogenesis. For example, epidermal growth factor receptor (EGFR) inhibitors can inhibit tumor cell proliferation and survival and are used to treat breast cancer and non-small cell lung cancer [20]. CDK4/6 inhibitors can disrupt the cell cycle of tumor cells, preventing cell division and proliferation, and play an important role in the treatment of breast cancer [21]. Vascular endothelial growth factor receptor (VEGFR) inhibitors can interfere with tumor angiogenesis and are widely used to treat various types of tumors [22]. Therefore, exploring the molecular biology mechanisms of tumor occurrence and development and clarifying key molecules related to malignant tumor occurrence are of great significance for expanding the scope of targeted therapy and improving its effectiveness.

CircRNAs are a type of noncoding RNA molecules that, unlike linear RNAs, form a closed-loop structure in which their ends are joined together by covalent bonds, forming a stable circular structure. In recent years, circRNAs have attracted widespread attention in tumor biology [23]. Studies have shown that circRNAs are involved in promoting or inhibiting various biological processes in malignant tumors, such as proliferation, metastasis, invasion, and drug resistance. For example, circ_0003356 is downregulated in gastric cancer and can inhibit the proliferation, invasion, migration, and epithelial-mesenchymal transition (EMT) process of gastric cancer cells, inducing apoptosis [24]. CircMAN1A2 is upregulated in nasopharyngeal carcinoma and can promote the proliferation, invasion, angiogenesis, and tumorigenesis of nasopharyngeal carcinoma cells [25]. There are also relevant reports on gliomas, such as the high expression of circular RNA XRCC5 in gliomas, which aggravates glioma progression [26]. CircPKD2 is significantly downregulated in gliomas and inhibits glioma cell proliferation, invasion, and glycolytic metabolism [27]. In this study, through circRNA sequencing analysis and examination of clinical specimens, we confirmed that circGRIK2 was significantly upregulated in gliomas, and its levels further increased with higher WHO grades. Further functional experiments confirmed that circGRIK2 was involved in glioma cell proliferation, invasion, migration, and tumorigenesis. Therefore, the primary aim of this study was to confirm that circGRIK2 was a novel oncogene related to gli-

oma occurrence and development and participating in malignant progression of gliomas, thus having certain clinical research significance and value.

CircRNAs can influence the function and expression regulatory networks of tumor cells through various mechanisms. First, circRNAs can act as sponges for miRNAs, forming circRNA-miRNA complexes that sequester miRNA molecules and release mRNA molecules from miRNA-mediated regulation, thus affecting gene expression in cells [28]. For example, circNDC80 upregulates the expression of ECE1 by sponging miR-139-5p in glioblastoma, promoting its malignant progression and tumorigenesis [29]. Second, circRNAs can interact with proteins, influencing cell signaling pathways and regulatory factors. For instance, circNEIL3 promotes glioma progression and exosome-mediated macrophage immunosuppressive polarization by stabilizing IGF2BP3 [30]. Furthermore, some circRNAs have coding potential for small peptides or possess splice regulatory functions, allowing them to regulate alternative splicing of genes. Although the roles of circRNAs in malignant tumors have been widely studied, the understanding of their specific mechanisms and regulatory networks is still relatively limited.

In this study, we analyzed the potential oncogenic mechanisms of circGRIK2. We primarily focused on studying circGRIK2 as a sponge that can bind to specific miRNAs. We discovered that circGRIK2 could sponge and adsorb miR-1303, and the anticancer effect of circGRIK2 silencing could be blocked by an inhibitor of miR-1303. MiR-1303 is a small RNA molecule that has not been extensively studied in gliomas but has been reported in other malignant tumors. In osteosarcoma, miR-1303 is downregulated and exerts its effects by targeting FGF7, which leads to the inhibition of cell proliferation, cell cycle arrest, and suppression of the EMT process [31]. In clear cell renal cell carcinoma, miR-1303 is involved in promoting cell proliferation and inhibiting cell apoptosis through regulation of the miR-1303-p/STARD9 axis [32]. However, in acute myeloid leukemia, miR-1303 acts as an oncogene, promoting cancer cell proliferation and inhibiting apoptosis [33]. In non-small cell lung cancer, miR-1303 is significantly upregulated, and its high expression is associated with a shortened patient survival time. Moreover, overexpression of miR-1303 promotes cell proliferation, migration, and invasion [34]. These contrasting results suggest that miR-1303 may have different biological roles in different tumors. In gliomas, our research suggests that miR-1303 has an anticancer effect and plays a role in inhibiting malignant progression of glioma cells.

Subsequent studies to further explore the downstream genes regulated by circGRIK2 through miR-1303 sponging indicated that miR-1303 targeted and regulated HOXA10. Overexpression of circGRIK2 sequestered miR-1303, preventing the miR-1303-mediated degradation of HOXA10 and leading to its upregulation. Additionally, the inhibitory effect of circGRIK2 silencing on malignant progression of glioma could be restored by overexpressing HOXA10. HOXA10, as a transcription factor, has been reported to play a clear biological role in gliomas and several other malignancies. In gliomas, the long noncoding RNA PSMA3-AS1 promotes tumor progression through upregulation of HOXA10, while silencing HOXA10 hampers glioma cell proliferation and induces apoptosis [35]. In pediatric glioblastoma, phosphoinositide 3-kinase-mediated expression of HOXA9/HOXA10 contributes to MGMT-independent temozolomide resistance [36]. In hepatocellular carcinoma, miR-135a inhibits cell proliferation by downregulating HOXA10, while HOXA10 promotes malignant progression of liver cancer [12]. LncRNA HOXA10-AS promotes the progression of esophageal carcinoma by regulating the expression of HOXA10 [37]. HOXA10 enhances cell proliferation and suppresses apoptosis in esophageal cancer through activation of the p38/ERK signaling pathway [38]. CircKIAA0368 promotes proliferation, migration, and invasion of nasopharyngeal carcinoma by upregulating HOXA10 [39]. Furthermore, HOXA10 methylation is mainly present in high-grade gliomas, especially glioblastomas, and high levels of HOXA10 methylation indicate a relatively favorable prognosis for patients [40]. Therefore, the oncogenic role of circGRIK2 and its interaction with HOXA10, discovered in this study, align with previous research findings, confirming the reliability of our results. However, there is still limited research on the downstream mechanisms of

oncogenic effects of HOXA10, and further in-depth investigations are needed.

To further explore the role of the high expression of circGRIK2 in glioma, we analyzed the RNA-binding proteins (RBPs) that could bind to circGRIK2. RBPs are a class of proteins that can interact with and bind to RNA molecules [41]. RBPs play various important functions in cells, including the regulation of RNA transcription, splicing, stability, localization, and translation processes [42]. RBPs can recognize and bind to specific regions of RNA sequences, which can include the RNA secondary structure, specific sequences, or specific structural domains [43]. By binding to RNA, these proteins can regulate the function, processing, transport, and interaction of RNA with other proteins. The function of RBPs is crucial in the normal physiological processes of cells and is closely associated with various diseases, including cancer, neurological disorders, and genetic diseases [44]. In this study, EIF4A3 was identified as the RBP that could bind to circGRIK2. EIF4A3 is a widely reported RBP that has been shown to promote multiple malignancies, including glioblastoma, lung cancer, and breast cancer [45, 46]. It is involved in the formation and maintenance of circular RNAs. For example, eukaryotic initiation factor 4A-3 promotes glioblastoma growth and invasion through the Notch1-dependent pathway [47]. CircCABIN1 can be cyclized by EIF4A3 and can lead to temozolomide resistance in glioblastoma by sustaining ErbB downstream signaling [48]. EIF4A3 induces circCCNB1 expression in glioma and participates in glioma progression by elevating CCND1 levels through interaction with miR-516b-5p and HuR [49]. In this study, we found that EIF4A3 could bind to circGRIK2, participate in maintaining its stability, and upregulate the expression of circGRIK2 in glioma. This explains the reason for the high expression of circGRIK2 in glioma.

In summary, our study identified a novel circular RNA, circGRIK2, which is associated with the occurrence and development of glioma. Our study explored the potential molecular mechanisms of circGRIK2 and found that it acted as an oncogene by competitively sponging miR-1303 and upregulating the oncogene and transcription factor HOXA10. In addition, the RNA-binding protein EIF4A3 could bind to and stabilize circGRIK2, leading to its high expression in glioblastoma. The discovery of circGRIK2 not only enhances our understanding of the roles of circular RNAs in the tumorigenesis and progression of glioma but also provides a new target for molecular targeted therapy of glioma.

Acknowledgements

This work was supported by the National Natural Science Foundation of China (grant number 81902531).

Written informed consent was obtained from all enrolled patients.

Disclosure of conflict of interest

None.

Abbreviations

NcRNAs, non-coding RNAs; circRNA, circular RNA; miRNAs, microRNAs; ceRNAs, competing endogenous RNAs; NBT, normal brain tissues; NHA, normal human astrocytes; H&E stain, hematoxylin and eosin stain; IHC, Immunohistochemistry; qRT-PCR/qPCR, Real-Time Quantitative Reverse Transcription polymerase chain reaction; RISC, RNA-induced silencing complex; 3'UTR, 3' untranslated region; MRE, miRNA response elements; Ago2, Argonaute 2; RIP assays, RNA immunoprecipitation assays; RBPs, RNA-binding proteins.

Address correspondence to: Xinrui Du, Department of Neurosurgery, Zibo Central Hospital, Zibo 255036, Shandong, China. E-mail: dxr1614@163.com

References

[1] Bianconi A, Palmieri G, Aruta G, Monticelli M, Zeppa P, Tartara F, Melcarne A, Garbossa D and Cofano F. Updates in glioblastoma immunotherapy: an overview of the current clinical and translational scenario. Biomedicines 2023; 11: 1520.

[2] Huang Q, Pan X, Zhu W, Zhao W, Xu H and Hu K. Natural products for the immunotherapy of glioma. Nutrients 2023; 15: 2795.

[3] Bernhard C, Reita D, Martin S, Entz-Werle N and Dontenwill M. Glioblastoma metabolism: insights and therapeutic strategies. Int J Mol Sci 2023; 24: 9137.

[4] Bhargav AG, Domino JS, Alvarado AM, Tuchek CA, Akhavan D and Camarata PJ. Advances in computational and translational approaches for malignant glioma. Front Physiol 2023; 14: 1219291.
[5] Ji X, Ding W, Wang J, Zhou B, Li Y, Jiang W, Pan H, Gu J and Sun X. Application of intraoperative radiotherapy for malignant glioma. Cancer Radiother 2023; 27: 425-433.
[6] Ahmed SP, Castresana JS and Shahi MH. Role of circular RNA in brain tumor development. Cells 2022; 11: 2130.
[7] Chen M, Yan C and Zhao X. Research progress on circular RNA in glioma. Front Oncol 2021; 11: 705059.
[8] Dou Y, Tian W, Wang H and Lv S. Circ_0001944 contributes to glycolysis and tumor growth by upregulating NFAT5 through acting as a decoy for miR-142-5p in non-small cell lung cancer. Cancer Manag Res 2021; 13: 3775-3787.
[9] Jiang Y, Zhao J, Liu Y, Hu J, Gao L, Wang H and Cui D. CircKPNB1 mediates a positive feedback loop and promotes the malignant phenotypes of GSCs via TNF-α/NF-κB signaling. Cell Death Dis 2022; 13: 697.
[10] Jiang Y, Zhao J, Li R, Liu Y, Zhou L, Wang C, Lv C, Gao L and Cui D. CircLRFN5 inhibits the progression of glioblastoma via PRRX2/GCH1 mediated ferroptosis. J Exp Clin Cancer Res 2022; 41: 307.
[11] Feng S, Wang K, Shao Z, Lin Q, Li B and Liu P. MiR-373/miR-520s-CD44 axis significantly inhibits the growth and invasion of human glioblastoma cells. Arch Med Res 2022; 53: 550-561.
[12] Lin J, Lian X, Xue S, Ouyang L, Zhou L, Lu Y and Xie L. miR-135a inhibits the proliferation of HBV-infected hepatocellular carcinoma cells by targeting HOXA10. Transl Cancer Res 2023; 12: 135-149.
[13] Zhou J, Wang C, Liu Y, Cui D, Wang Z, Jiang Y and Gao L. Circular RNA circPTPRF promotes the progression of GBM via sponging miR-1208 to up-regulate YY1. Cancer Cell Int 2022; 22: 359.
[14] Yan Y, Wang H, Hu J, Guo T, Dong Q, Yin H, Yuan G and Pan Y. CircRNA-104718 promotes glioma malignancy through regulation of miR-218-5p/HMGB1 signalling pathway. Metab Brain Dis 2023; 38: 1531-1542.
[15] Jiang Y, Zhou J, Hou D, Luo P, Gao H, Ma Y, Chen YS, Li L, Zou D, Zhang H, Zhang Y and Jing Z. Prosaposin is a biomarker of mesenchymal glioblastoma and regulates mesenchymal transition through the TGF-beta1/Smad signaling pathway. J Pathol 2019; 249: 26-38.
[16] Deng T, Liu Y, Yang Y, Yuan L, Liu F, Wang X, Zhang Q and Xie M. Regulation of microRNA miR-197-3p/CDC28 protein kinase regulatory subunit 1B (CKS1B) axis by circular RNA hsa_circ_0000285 promotes glioma progression. Bioengineered 2022; 13: 4757-4772.
[17] Jafarzadeh A, Noori M, Sarrafzadeh S, Tamehri Zadeh SS, Nemati M, Chatrabnous N, Jafarzadeh S, Hamblin MR, Jafari Najaf Abadi MH and Mirzaei H. MicroRNA-383: a tumor suppressor miRNA in human cancer. Front Cell Dev Biol 2022; 10: 955486.
[18] Wang K, Pan S, Zhao P, Liu L, Chen Z, Bao H, Wang H, Zhang Y, Zhuge Q and Yang J. PTBP1 knockdown promotes neural differentiation of glioblastoma cells through UNC5B receptor. Theranostics 2022; 12: 3847-3861.
[19] Skouras P, Gargalionis AN and Piperi C. Exosomes as novel diagnostic biomarkers and therapeutic tools in gliomas. Int J Mol Sci 2023; 24: 10162.
[20] Nasrolahi A, Azizidoost S, Radoszkiewicz K, Najafi S, Ghaedrahmati F, Anbiyaee O, Khoshnam SE, Farzaneh M and Uddin S. Signaling pathways governing glioma cancer stem cells behavior. Cell Signal 2023; 101: 110493.
[21] Rodríguez Y, Unno K, Truica MI, Chalmers ZR, Yoo YA, Vatapalli R, Sagar V, Yu J, Lysy B, Hussain M, Han H and Abdulkadir SA. A genome-wide CRISPR activation screen identifies PRRX2 as a regulator of enzalutamide resistance in prostate cancer. Cancer Res 2022; 82: 2110-2123.
[22] Wu HB, Yang S, Weng HY, Chen Q, Zhao XL, Fu WJ, Niu Q, Ping YF, Wang JM, Zhang X, Yao XH and Bian XW. Autophagy-induced KDR/VEGFR-2 activation promotes the formation of vasculogenic mimicry by glioma stem cells. Autophagy 2017; 13: 1528-1542.
[23] Fan J, Wang Y, Liang X, Zhou F, Li S, Li X and Li Y. Roles of circular RNAs in regulating the development of glioma. J Cancer Res Clin Oncol 2023; 149: 979-993.
[24] Li WD, Wang HT, Huang YM, Cheng BH, Xiang LJ, Zhou XH, Deng QY, Guo ZG, Yang ZF, Guan ZF and Wang Y. Circ_0003356 suppresses gastric cancer growth through targeting the miR-668-3p/SOCS3 axis. World J Gastrointest Oncol 2023; 15: 787-809.
[25] Mo H, Shen J, Zhong Y, Chen Z, Wu T, Lv Y, Xie Y and Hao Y. CircMAN1A2 promotes vasculogenic mimicry of nasopharyngeal carcinoma cells through upregulating ERBB2 via sponging miR-940. Oncol Res 2023; 30: 187-199.
[26] Tan LM, Chen P, Nie ZY, Liu XF and Wang B. Circular RNA XRCC5 aggravates glioma progression by activating CLC3/SGK1 axis via recruiting IGF2BP2. Neurochem Int 2023; 166: 105534.
[27] Liu F, Wu H, Wu G, Long J, Dai J and Wang Z. circPKD2 inhibits the glioma cell proliferation, invasion and glycolytic metabolism through regulating the miR-1278/LATS2 axis. Neurosci Lett 2023; 801: 137126.
[28] Xiao G, Yu L, Tan W, Yang H, Li W, Xia R and Li Y. Propofol inhibits glioma progression by regulating circMAPK4/miR-622/HOXA9 axis. Metab Brain Dis 2023; 38: 233-244.

[29] Wang Y, Wang B, Zhou F, Lv K, Xu X and Cao W. CircNDC80 promotes glioblastoma multiforme tumorigenesis via the miR-139-5p/ECE1 pathway. J Transl Med 2023; 21: 22.
[30] Pan Z, Zhao R, Li B, Qi Y, Qiu W, Guo Q, Zhang S, Zhao S, Xu H, Li M, Gao Z, Fan Y, Xu J, Wang H, Wang S, Qiu J, Wang Q, Guo X, Deng L, Zhang P, Xue H and Li G. EWSR1-induced circNEIL3 promotes glioma progression and exosome-mediated macrophage immunosuppressive polarization via stabilizing IGF2BP3. Mol Cancer 2022; 21: 16.
[31] Han G, Guo Q, Ma N, Bi W, Xu M, Jia J and Wang W. LncRNA BCRT1 facilitates osteosarcoma progression via regulating miR-1303/FGF7 axis. Aging (Albany NY) 2021; 13: 15501-15510.
[32] Cheng T, Shuang W, Ye D, Zhang W, Yang Z, Fang W, Xu H, Gu M, Xu W and Guan C. SNHG16 promotes cell proliferation and inhibits cell apoptosis via regulation of the miR-1303-p/STARD9 axis in clear cell renal cell carcinoma. Cell Signal 2021; 84: 110013.
[33] Li L and Zhao W. The mutual regulatory loop between TPTEP1 and miR-1303 in leukemogenesis of acute myeloid leukemia. Cancer Cell Int 2021; 21: 260.
[34] Chen J, Jiang T, Yu B, Li T, Zhao P, Yuan L and Qi J. Upregulation of microRNA-1303 is a potential prognostic marker of non-small cell lung cancer. Cancer Biomark 2020; 28: 439-446.
[35] Huang T, Chen Y, Zeng Y, Xu C, Huang J, Hu W, Chen X and Fu H. Long non-coding RNA PSMA3-AS1 promotes glioma progression through modulating the miR-411-3p/HOXA10 pathway. BMC Cancer 2021; 21: 844.
[36] Gaspar N, Marshall L, Perryman L, Bax DA, Little SE, Viana-Pereira M, Sharp SY, Vassal G, Pearson AD, Reis RM, Hargrave D, Workman P and Jones C. MGMT-independent temozolomide resistance in pediatric glioblastoma cells associated with a PI3-kinase-mediated HOX/stem cell gene signature. Cancer Res 2010; 70: 9243-9252.
[37] Kuai J, Wu K, Han T, Zhai W and Sun R. LncRNA HOXA10-AS promotes the progression of esophageal carcinoma by regulating the expression of HOXA10. Cell Cycle 2023; 22: 276-290.
[38] Jiang L and Yang Q. HOXA10 enhances cell proliferation and suppresses apoptosis in esophageal cancer via activating p38/ERK signaling pathway. Open Med (Wars) 2022; 17: 1750-1759.
[39] Chen Z, Gong Q, Li D and Zhou J. CircKIAA0368 promotes proliferation, migration, and invasion by upregulating HOXA10 in nasopharyngeal carcinoma. Am J Rhinol Allergy 2022; 36: 615-627.
[40] Di Vinci A, Casciano I, Marasco E, Banelli B, Ravetti GL, Borzì L, Brigati C, Forlani A, Dorcaratto A, Allemanni G, Zona G, Spaziante R, Gohlke H, Gardin G, Merlo DF, Mantovani V and Romani M. Quantitative methylation analysis of HOXA3, 7, 9, and 10 genes in glioma: association with tumor WHO grade and clinical outcome. J Cancer Res Clin Oncol 2012; 138: 35-47.
[41] Luo P, Gong Y, Weng J, Wen F, Luo J, Hu C, Xiao J and Shu J. CircKIF4A combines EIF4A3 to stabilize SDC1 expression to activate c-src/FAK and promotes TNBC progression. Cell Signal 2023; 108: 110690.
[42] Zhang Y, Qi W and Wu Y. EIF4A3-induced circular RNA SCAP facilitates tumorigenesis and progression of non-small-cell lung cancer via miR-7/SMAD2 signaling. Environ Sci Pollut Res Int 2023; 30: 65237-65249.
[43] Yu W, Liang J, Fang T, Jiang J, Zhao R, Li R, Han J and Tian H. EIF4A3 acts on the PI3K-AKT-ERK1/2-P70S6K pathway through FLOT1 to influence the development of lung adenocarcinoma. Mol Cancer Res 2023; 21: 713-725.
[44] Meng X, Li W, Meng Z and Li Y. EIF4A3-induced circBRWD3 promotes tumorigenesis of breast cancer through miR-142-3p_miR-142-5p/RAC1/PAK1 signaling. BMC Cancer 2022; 22: 1225.
[45] Lu L, Zeng Y, Yu Z, Chen S, Xie J, Rao B, Yang B, Qiu F, Lu J and Yang L. EIF4a3-regulated circRABL2B regulates cell stemness and drug sensitivity of lung cancer via YBX1-dependent downregulation of MUC5AC expression. Int J Biol Sci 2023; 19: 2725-2739.
[46] Huang X, Tan W, Liu Z, Fu X, Li Z, Lai S, Li Q, Zhong X, Qu F, Zhang H and Li H. EIF4A3-induced circZFAND6 promotes breast cancer proliferation and metastasis through the miR-647/FASN axis. Life Sci 2023; 324: 121745.
[47] Wei L, Pan M, Jiang Q, Hu B, Zhao J, Zou C, Chen L, Tang C and Zou D. Eukaryotic initiation factor 4 A-3 promotes glioblastoma growth and invasion through the Notch1-dependent pathway. BMC Cancer 2023; 23: 550.
[48] Liu X, Guo Q, Gao G, Cao Z, Guan Z, Jia B, Wang W, Zhang K, Zhang W, Wang S, Li W, Hao Q, Zhang Y, Li M, Zhang W and Gu J. Exosome-transmitted circCABIN1 promotes temozolomide resistance in glioblastoma via sustaining ErbB downstream signaling. J Nanobiotechnology 2023; 21: 45.
[49] Li X, Wang C, Chen G, Zou W, Deng Y and Zhou F. EIF4A3-induced circCCNB1 (hsa_circ_0001495) promotes glioma progression by elevating CCND1 through interacting miR-516b-5p and HuR. Metab Brain Dis 2022; 37: 819-833.

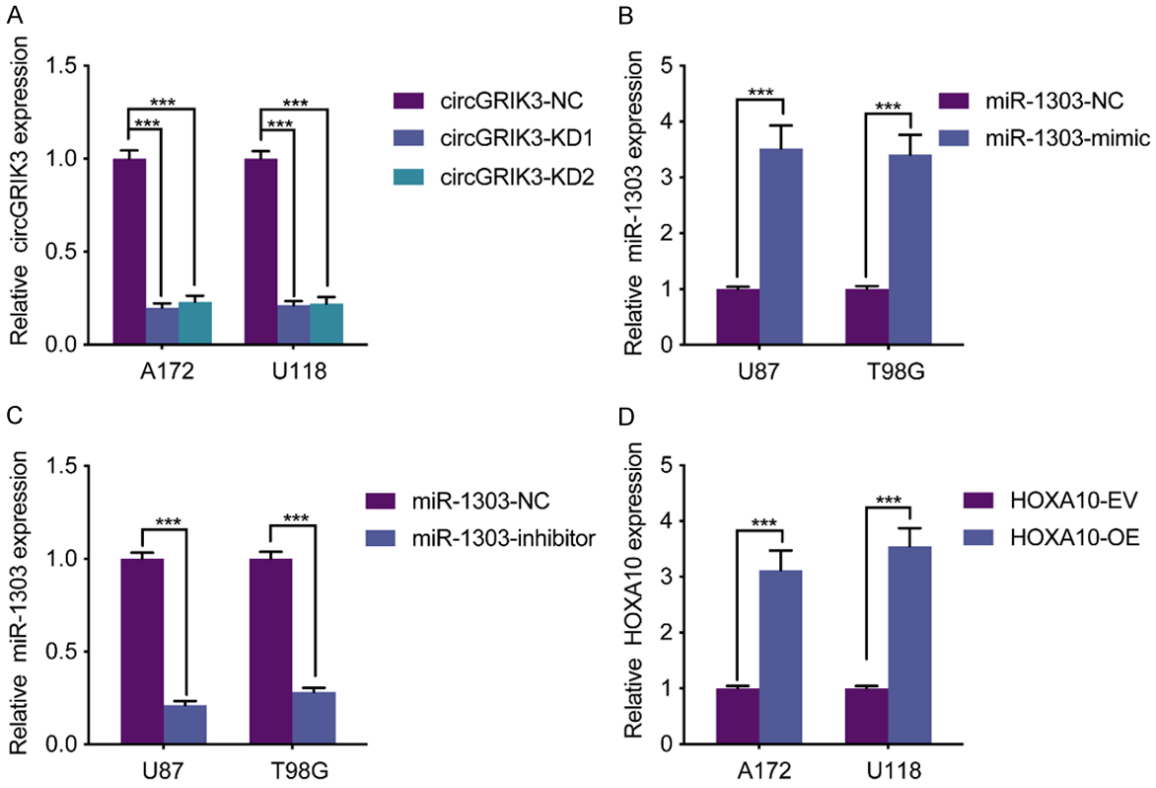

Supplementary Figure 1. The transfection efficiency of targeted genes in glioma cells were confirmed. (A) qPCR confirmed the transfection efficiency of circGRIK2 silence in glioma cells U118 and A172. (B, C) qPCR confirmed the transfection efficiency of -1303-mimic (B) or miR-1303-inhibitor (C) treatment in glioma cells U87 and T98G. (D) qPCR confirmed the transfection efficiency of HOXA10 overexpression in glioma cells U118 and A172.

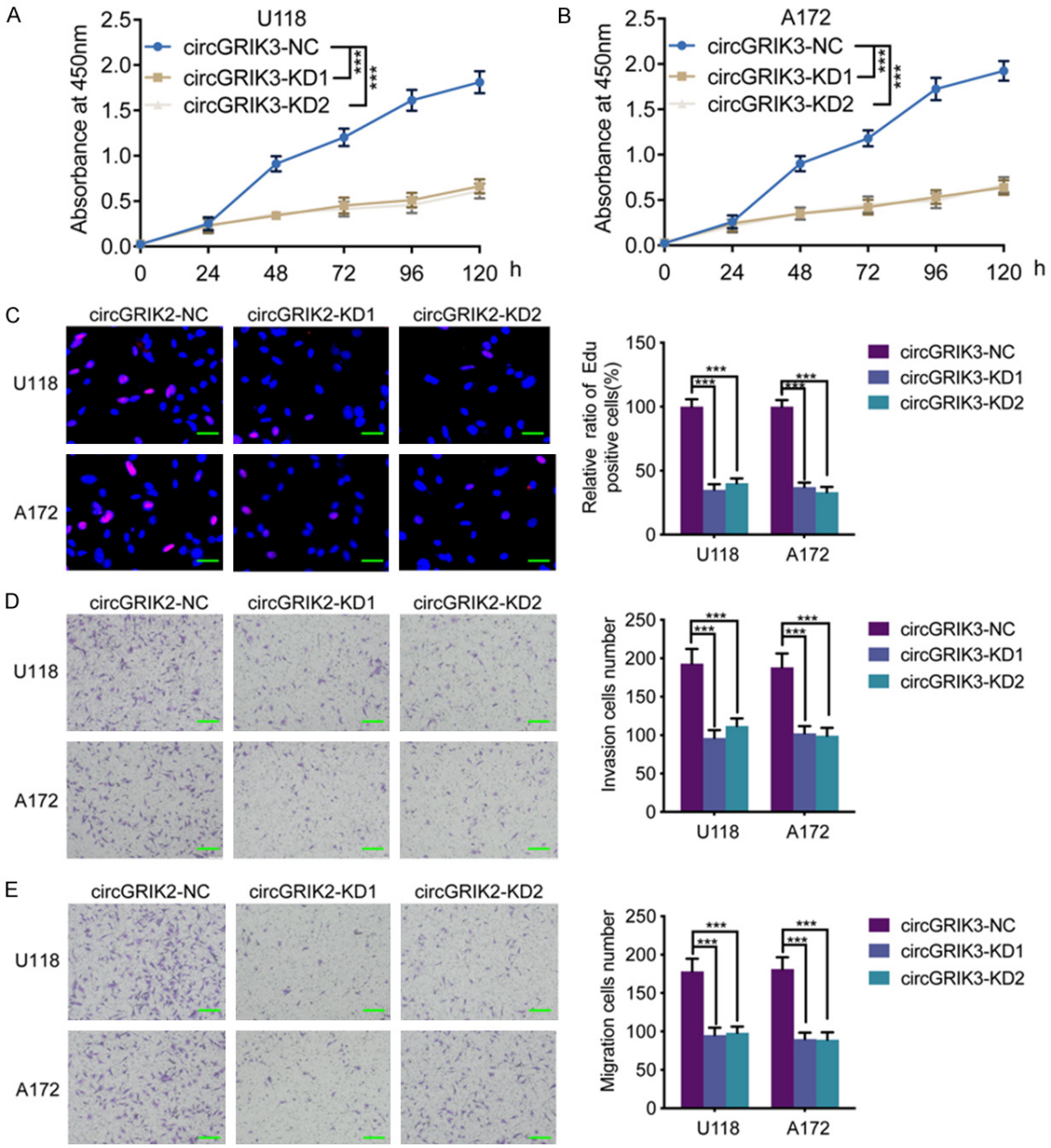

Supplementary Figure 2. CircGRIK2 knockdown inhibited the proliferation and invasion in glioma cells. (A, B) MTS assays were performed to assess the changes in cell viability of U118 and A172 glioma cell lines after circGRIK2 knockdown. (C) EdU assays were conducted to evaluate the changes in the percentage of EdU-positive cells in U118 and A172 glioma cell lines following circGRIK2 knockdown. Scale bar = 50 μm. (D, E) Transwell (D) and cell migration (E) assays were performed to examine the alterations in the number of invaded and migrated cells in U118 and A172 glioma cell lines upon circGRIK2 knockdown. Scale bar = 50 μm. All data are shown as the mean ± SD (three independent experiments). **P < 0.05; **P < 0.01; ***P < 0.001.*